PAPER • OPEN ACCESS

Implications of T loss in first wall armor and structural materials on T-self-sufficiency in future burning fusion devices

To cite this article: K. Schmid *et al* 2024 *Nucl. Fusion* **64** 076056

OPEN ACCESS
IOP Publishing | International Atomic Energy Agency
Nuclear Fusion
Nucl. Fusion **64** (2024) 076056 (11pp)
https://doi.org/10.1088/1741-4326/ad52a7

Implications of T loss in first wall armor and structural materials on T-self-sufficiency in future burning fusion devices

K. Schmid[1,*], T. Schwarz-Selinger[1], R. Arredondo[1], A. Theodorou[1] and T. Pomella Lobo[2]

[1] Max-Planck-Institut for Plasma Physics, Garching, Germany
[2] Institute for Neutron Physics and Reactor Technology, Karlsruhe Institute of Technology (KIT), Eggenstein-Leopoldshafen, Germany

E-mail: Klaus.Schmid@ipp.mpg.de

Received 9 January 2024, revised 6 May 2024
Accepted for publication 31 May 2024
Published 13 June 2024

Abstract

Future fusion reactors will have to breed enough tritium (T) to sustain continuous operation and to produce excess T to power up other fusion reactors. Therefore, T is a scarce resource that must not be lost inside the fusion power plants systems. The factor that describes the T production is the 'tritium breeding ratio' (TBR) which is the ratio of the breading rate in atoms per second to the burn rate in atoms per second. Its value is calculated from neutronics analyses of the breeding process in the blanket and coupled dynamics of the T processing plant. However, these calculations generally ignore the T transport and loss in the first wall by assuming essentially instantaneous recycling of the impinging T in-flux. In this paper the transport and retention of T in the main chamber first wall of a future EU-DEMO reactor is investigated based on the available material data and expected particle loads onto the wall. Two breeding blanket concepts are compared WCLL (water cooled lithium lead) and HCPB (helium cooled pebble bed) and the resulting wall-loss probabilities are compared with a simple balance model that describes the maximum allowable wall loss given a TBR to achieve T-self-sufficiency.

Keywords: T-self-sufficiency, tungsten, EUROFER, diffusion-trapping modeling

(Some figures may appear in colour only in the online journal)

1. Introduction

In future burning fusion devices, the ability to breed enough tritium (T) to sustain continuous operation and to produce fuel for start-up of additional fusion devices will be a key criterion for achieving net energy production by nuclear fusion. This paper will touch on the current level of understanding of trapping of hydrogen isotopes (HIs) in the reduced activation ferritic martensitic steel EUROFER and tungsten (W). This available data is then used to make modeling predictions on T transport and trapping in the first wall of the EU-DEMO. Finally, the implications of the resulting T wall lost probability on T-self-sufficiency is discussed. These current results suggest that losses of T in the wall may delay achieving T-self-sufficiency for several years, maybe even beyond the lifetime of the breeding blanket [1].

* Author to whom any correspondence should be addressed.

The T production is governed by the 'tritium breeding ratio' TBR which denotes the number of tritium atoms bred in the breeding blanket per neutron produced by the deuterium/tritium fusion reaction. The TBR is commonly computed by Monte-Carlo codes (e.g. MCNP) that provide the nuclear response of complex structures under irradiation [2]. The impacts of this parameter, such as the necessary efficiency of T extraction & recovery systems [3] or safety concerns due to the amounts of tritiated exhaust handled by the vacuum systems, are usually assessed with systems-level analyses performed by systems-codes (e.g. MIRA [4]) or more dedicated design tools (e.g. EcosimPro [5]).

However, these calculations generally ignore the loss of T via retention in the first wall and structural material by neglecting n-irradiation induced traps [6]. It is generally assumed that T quickly recycles back into the plasma from the tungsten (W) surfaces and permeates quickly through EUROFER-based structural materials into the coolant, where T can be recovered. However, recent computer simulations, based on experimental data for both W and EUROFER, suggest that the defects produced by displacement damage from fast fusion neutrons in these materials will effectively trap T atoms and either only release them at very high temperatures and/or significantly slow down permeation to the coolant. This retention of T in the first wall and slowing down of permeation results in a time delay for the achievement of T-self-sufficiency of several years and might even delay it beyond the lifespan of the blanket. Further, the increase in the total T inventory could become a licensing issue [7].

The influence of T-wall-loss on the achievement of T-self-sufficiency was first addressed in [8, 9] where a simple balance model of T production vs. loss to the wall was introduced. They already show the need for an extremely low T-wall-loss, which rules out low-Z wall elements and only leaves high-Z elements as potential first wall materials. However, these publications do not include a time dependence and hence cannot reflect that the propagation of the diffusion front reduces over time, due to flatting of the concentration gradient. Therefore, in [1] the initial model was improved, allowing to compare the time evolution of the T-wall-loss probability $P_{\mathrm{Wall}}(t)$ with the required level $P_{\mathrm{Wall}}^{\mathrm{Crit}}$ for T-self-sufficiency. The value of $P_{\mathrm{Wall}}^{\mathrm{Crit}}$ depends on the assumptions on the TBR and fuelling efficiencies that enter the simple balance model as outlined in [1]. The time evolution of $P_{\mathrm{Wall}}(t)$ depends on the assumptions of particle fluxes and temperatures resulting from the applied blanket concepts. Depending on the input choices $P_{\mathrm{Wall}}(t)$ spans a wide range which may eventually overlap with range of values for $P_{\mathrm{Wall}}^{\mathrm{Crit}}$. This overlap on average occurs approximately within the first two years, but it may take up to six years, because large amounts of T are needed to saturate the wall before T permeates through the wall and becomes recoverable.

The calculated $P_{\mathrm{Wall}}(t)$ data from [1] depends on numerous assumptions on particle fluxes and energies and wall temperature gradients that were taken from the current EU-DEMO design [10]. However, the main uncertainties in the calculation of $P_{\mathrm{Wall}}(t)$ are due to the parameters describing the T trapping in W and EUROFER. These have been the focus of numerous experiments performed within the EUROfusion work package on plasma–wall interaction [11] over the recent years. The formation of trap sites in W under displacement damage by fusion neutrons was investigated both experimentally and by modeling in [12–14]. It was found that the trap concentration quickly saturates at displacement per atom levels of 0.1. The saturation concentration depends on temperature but also on the presence of HIs and He. Both, His and He strongly increase the maximum trapped concentration of His up to levels of several 10^{-2} His trapped per W atom, which is at least two to three orders of magnitude larger than retention in un-damaged W. Annealing the displacement damaged W at first-wall operation temperature of the order of 600–800 K reduces the maximum trapped concentration of His only by a factor two thus allowing to retain large amounts of His after cool down. The database on trapping in W has evolved significantly over the past years. However, for displacement-damaged EUROFER the database is rather sparse. First results [15, 16] suggest that EUROFER behaves similar to W under displacement damage in so far as the trap site concentration increases and that the presence of His and He further increase the maximum trapped concentration of His by a factor two each. However, for low temperature operation the concentration of trapped HIs in EUROFER is a factor 100 lower than in W [16]. Also results from [15, 16] suggest that displacement generated traps in EUROFER anneal at 600 K and only the weak intrinsic traps remain. However first unpublished results suggest that the presence of He, which would result from transmutation in a fusion reactor, stabilizes the displacement damage induced trap sites. Therefore, as the knowledge base on EUROFER increases these predictions will need to be further be refined. The current values on the expected retention in EUROFER should be seen as a lower boundary.

For this paper the calculations from [1] are partially repeated based on a more refined material database both for W and EUROFER. The wall loss probability $P_{\mathrm{Wall}}(t)$ is calculated for the two breeding blanket concepts WCLL (water cooled lithium lead) and HCPB (helium cooled pebble bed) that are foreseen for DEMO. Also, for the refined material database a comparison of $P_{\mathrm{Wall}}(t)$ with $P_{\mathrm{Wall}}^{\mathrm{Crit}}$ qualitatively shows the same results as in [1]: depending on the wall fluxes and temperature expected for the blanket designs it may take years to achieve T-self-sufficiency. In addition, also the effect of potentially pre-saturating the first wall with D was investigated. However, due to strong isotope exchange no significant difference to the non-pre-saturated case could be found.

2. Simulation setup

As in [1] the diffusion trapping code TESSIM-X [17, 18] is used for the calculation of $P_{\mathrm{Wall}}(t)$. Two breeding blanket designs were considered in the calculations WCLL [19] and HCPB [20]. Both are based on a W armor layer facing the plasma on top of a EUROFER layer which is in contact with

Table 1. EUROFER and tungsten material thicknesses and resulting temperatures for the two blanket coolant concepts.

Design	$\Delta X_{\mathrm{Tungsten}}$ (mm)	$\Delta X_{\mathrm{EUROFER}}$ (mm)	T_{Surface} (K)	$T_{\mathrm{Interface}}$ (K)	T_{Coolant} (K)
HCPB	2	2	792	783	683
HCPB0.8W3.2FE	0.8	3.2	792	789	683
WCLL	2	3	673	663	612
WCLL0.8W4.2FE	0.8	4.2	673	669	612

the coolant. In the context of the simulation the designs only differ in the thicknesses of the W and EUROFER layers and the resulting temperature profiles. The different layer thicknesses and resulting temperatures are summarized in table 1. Linear temperature profiles are assumed in between the surface, the W/EUROFER interface and toward the coolant.

The different $\Delta X_{\mathrm{Tungsten}}$ values result from trying to better mimic the fact that the W armor layer is joined to the EUROFER structural and coolant layer by a functionally graded material (FGM) interlayer which only contains 0.8 mm of pure W followed by graded transition to EUROFER. However, as also explained in [1] such an FGM is currently beyond the scope of modeling due to a lack of material parameters (diffusivities, solubilities and trap concentrations, energies and frequency factors) needed for diffusion trapping modeling of T transport through the FGM.

Different from [1] the trapping of D, T in W and EUROFER was modeled using the fill-level-dependent trapping picture (see [17] for details). The details of the trapping parameters used for W and EUROFER are described in sections 2.1 and 2.2 respectively. The boundary at the plasma-facing W surface was modeled as a Dirichlet type diffusion limited boundary. This choice is based on the extensive modeling on D uptake and release from W as part of determining the trapping parameters for W in section 1.1. For the W/EUROFER interface the concentration of solute D, T on each side of the interface is based on two equations. Material conservation requires equal diffusion fluxes on both sides of the interface. Furthermore, an equilibrium of the chemical potentials of solute D and T at the interface was assumed which is described by the ratios of solute concentrations on each side of the interface being equal to the ratio of solubilities. The solubility in W was thereby taken from [21] and the solubility in EUROFER from [22]. For the material conservation equation, the required solute diffusion coefficients were taken from [23] for W and from [22] for EUROFER. The solute diffusion coefficients for D (D_{D}) and T (D_{T}) differ due to the different atomic mass: $D_{\mathrm{T}} = \sqrt{2/3} D_{\mathrm{D}}$. This mass-ratio scaling is based on the results for the solute diffusion coefficients of H and D in [23]. From EUROFER towards the coolant two types of boundary conditions are compared: diffusion-limited and surface-limited boundary conditions. For the surface-limited boundary conditions the Pick–Sonnenberg surface model option in TESSIM-X was used (see [18] for details) and the various required activation energies for the near surface energy landscape are taken from modeling the D uptake into EUFOFER from plasma and gas phase as described in [24]. While in [24] the uptake from plasma and gas phase is modeled, the resulting near surface energy landscape also affects the release of D and T from EUROFER. Since the EUROFER/water boundary condition is unknown both diffusion- and surface-limited boundaries are applied in the parameter scan. However, it was found that the EUROFER/water boundary has essentially no influence on the result which is dominated by the W armor layer.

The incident flux Γ_{In} of D and T was varied from 10^{18} to 10^{20} ($\mathrm{m}^{-2}\ \mathrm{s}^{-1}$) assuming a 50:50 mixture of D and T. In contrast to [1], true co-permeation including isotope exchange between trapped and solute HIs of different type is simulated. The assumption is made that the average particle impact energy is 500 eV which is based on both influx due to charge exchange neutrals [25] and potential influx of ions due to filamentary transport [26]. In the context of the simulation, varying the impact energy results in a different solute HI volume source term Φ_{Src} which is approximated by a Gaussian with centered at $R_{\mathrm{P}} = 9.8$ (nm) with a full width at half maximum of $\sigma_{\mathrm{Straggle}} = 10.8$ (nm). Only the non-reflected fraction $(1-R) \times \Gamma_{\mathrm{In}}$ of Γ_{In} thereby contributes to Φ_{Src}. Both the implantation range parameters R_{P} and $\sigma_{\mathrm{Straggle}}$ and the reflection coefficient $R = 0.54$ were calculated with SDTrimSP [27].

The total simulation time was set to $t_{\mathrm{SIM}} = 2 \times 108$ s corresponding to approximately 6 full power years (FPYs) of operation. For the calculation of $P_{\mathrm{Wall}}(t)$ all input parameters remained constant during t_{SIM}.

To investigate the potential beneficial effect of pre-saturating all defects with D and thus reduce retention of T, simulations are performed where the wall is first exposed to pure D for 2×108 s followed by another 2×108 s of again 50:50 D, T exposure. Apart from the varying influxes of D and T, all the other input parameters remained constant during the $2 \times t_{\mathrm{SIM}}$.

Finally, for all calculations $P_{\mathrm{Wall}}(t)$ is computed from the total retained amount $\delta^{\mathrm{T}}_{\mathrm{Ret}}\left(\mathrm{m}^{-2}\right)$ of T in the first wall divided by the total incident fluence $\theta^{\mathrm{T}}_{\mathrm{In}}$ of T where f_{T} is the flux fraction of T which equal to 0.5 except during pre-loading of the wall with D for the isotope exchange calculations,

$$\theta^{\mathrm{T}}_{\mathrm{In}} = \int f_{\mathrm{T}} \Gamma_{\mathrm{In}}\, \mathrm{d}t \left(\mathrm{m}^{-2}\right). \tag{1}$$

2.1. Trapping parameters in tungsten

The trapping parameters for W were determined by fitting the same experimental data taken from [28] that was also used in [29]. In [29] the thermal desorption spectra (TDS)

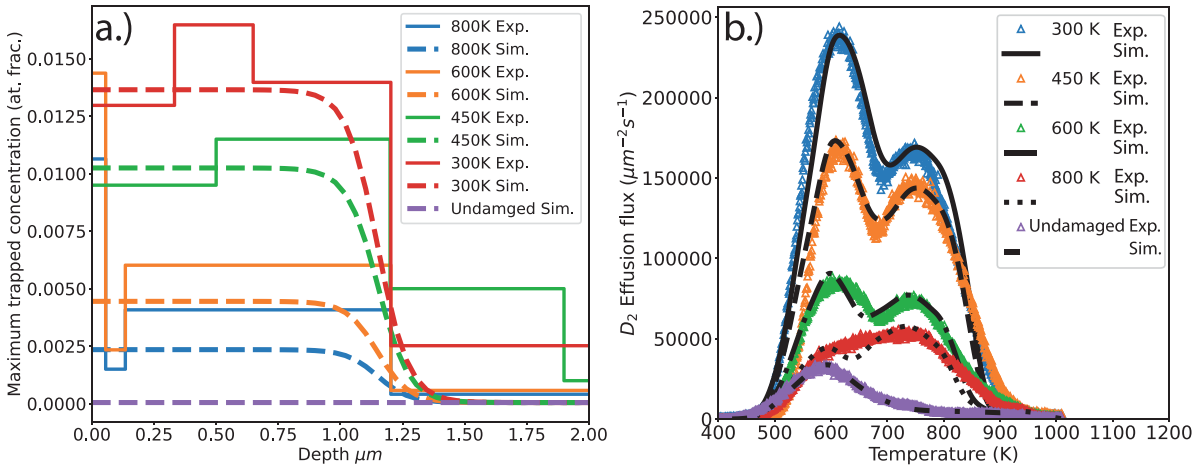

Figure 1. Comparison of measured (solid) and simulated (dashed) D depth profiles and TDS. The trapping rate parameters are the same for all temperatures only the near surface trap concentrations vary with temperature.

Table 2. Arrhenius rate parameters for trapping 'In' and de-trapping 'Out'.

Rate parameter	Trap 1	Trap 2	Trap 3 (intrinsic)
$\nu_{\mathrm{In}}\,(\mathrm{s}^{-1})$	4.5×10^{10}	4.5×10^{10}	4.5×10^{10}
$\Delta E_{\mathrm{In}}\,(\mathrm{eV})$	0.25	0.25	0.25
$\nu_{\mathrm{Out}}\,(\mathrm{s}^{-1})$	1.1×10^{11}	1.1×10^{11}	1.1×10^{11}
$\Delta E_{\mathrm{Out}}\,(\mathrm{eV})$	{1.57, 1.48}	{1.97, 1.94}	{1.34}

Similar to [29] traps 1 and 2 have two fill levels whereas trap 3 only has a single fill level.

of W samples, which were previously damaged by self-ion implantation at different temperatures and then loaded with D at 300 K, were simulated using the MHIMS code [30]. This combination of damaging at elevated temperatures and subsequent decoration of the defects by D implantation at low temperatures allows to determine the HI trap site concentration and the required rate parameters for diffusion trapping modeling of HI transport and retention in displacement damaged W. The reason for re-fitting this data is twofold: firstly, in [29] no unique set of rate parameters valid for all temperatures is given instead the data from each temperature is fitted separately and only a parameter range is finally given. Secondly, the applied code MHIMS uses a slightly different set of rate equations for fill-level-dependent trapping than the TESSIM-X code used in this work. Therefore, the results from [29] cannot directly be used here.

The trap concentration profiles were modeled according to the measured total trap profiles (see figure 1(*a*)) and the rate-model parameters were adjusted to match the TDS data (see figure 1(*b*)). To achieve the fits in figure 1 three different trap types were assumed. Following the measured data, the trap concentration profiles in figure 1(*a*) have a step-like structure with the near surface value being due to the displacement damage within the ion range of the 10.8 MeV W ions that remains at a given temperature. Since the samples were annealed at 2000 K prior to damaging their bulk trap concentration level is not affected by the temperatures during the self-ion implantation and thus the constant bulk level of trap sites is based on the fit to the undamaged case's TDS. The trap concentration levels for the different temperatures are summarized in table 3. The determined rate parameters, which are summarized in table 2, are the same for all temperatures, only the near-surface trap concentration was varied for fitting the TDS spectra of the samples damaged at different temperatures.

2.2. *Trapping parameters in EUROFER*

The trapping parameters for EUROFER where recently determined by fitting TDS spectra with TESSIM-X in [24]. The data fitted in [24] was taken from [15] where EUROFER samples were damaged at 300 K with 20 MeV W-ions and then loaded with D at 370 K to decorate the defects created by the displacement damage. The best fit was achieved with two defect types, one due to the displacement damage, located only at the surface within the depth range affected by the W-ion irradiation and the other intrinsic trapping site distributed homogeneously throughout the sample.

In contrast to the W data, the damaging was done at ambient temperatures and to assess the effect of temperature the samples were annealed after damaging at 600 K and 800 K (see [15]). This resulted in essentially full annealing the trap sites induced by the displacement damage whereas the intrinsic defects were not affected. However, other publications e.g. [6], where the damaging was performed at elevated temperatures, suggest the formation of voids which are known as strong traps for His. Therefore, the trap concentrations resulting from [15, 24] have to be understood as lower levels for the trap site concentration in radiation-damaged EUROFER. Since in this work trapping is dominated by the W layer, this potential underestimation of trapping in EUROFER does not

Table 3. Surface trap site concentrations (at. Frac.) for each trap and temperature during damaging. The trap concentrations for the undamaged case are constant throughout the sample and are also used as bulk level for the other cases.

Temperature/Case	Trap 1 concentration	Trap 2 concentration	Trap 3 concentration
800 K surface	1.5×10^{-4}	1.0×10^{-3}	4.0×10^{-5}
600 K surface	8.0×10^{-4}	1.4×10^{-3}	4.0×10^{-5}
450 K surface	2.2×10^{-3}	2.9×10^{-3}	4.0×10^{-5}
300 K surface	3.4×10^{-3}	3.4×10^{-3}	4.0×10^{-5}
Undamaged (=const. bulk-level)	3.5×10^{-6}	1.0×10^{-6}	4.0×10^{-5}

Table 4. Arrhenius rate parameters for trapping 'In' and de-trapping 'Out' determined in [24]. The trap concentration for trap 1 is for the case of damaging without subsequent annealing. After annealing above 600 K [15] the concentration of trap 1 is reduced to $\sim 1 \times 10^{-8}$ at. Frac. Whereas the concentration of trap 2 remains unchanged.

Parameter	Trap 1 (from displacement damage)	Trap 2 (intrinsic)
$\nu_{\mathrm{In}}\left(\mathrm{s}^{-1}\right)$	8.9×10^{12}	8.9×10^{12}
$\Delta E_{\mathrm{In}}\,(\mathrm{eV})$	0.15	0.15
$\nu_{\mathrm{Out}}\left(\mathrm{s}^{-1}\right)$	2.0×10^{13}	2.0×10^{13}
$\Delta E_{\mathrm{Out}}\,(\mathrm{eV})$	1.1	0.9
Trap concentration (at. Frac.)	2.5×10^{-3} (reduced to 1×10^{-8} above 600 K)	1×10^{-5}

affect the conclusions drawn. The rate parameters of two sites in EUROFER obtained in [24] are summarized in table 4.

It has to be understood that the trap parameters from [24] are also affected by the strong surface limit found in [24] for the uptake of His from the gas phase. The surface limit shifts the peaks during the TDS part of the simulation thus affecting the final values of the de-trapping energies and frequencies. Due to annealing the concentration of trap 1, which is due to displacement damage, is reduced from 2.5×10^{-3} to 1×10^{-8} (at. Frac.) for the simulations presented here, while the concentration of the intrinsic trap 2 is kept at 1×10^{-5} (at. Frac.) as suggested by the data in [15].

In comparison with previous work in [1] the refined modeling parameters for W and EUROFER differ mainly in the assumptions for EUROFER: the de-trapping energies for the most abundant trap are much lower (0.9 eV vs. 1.35 eV) and also the trap concentrations are significantly de-creased following the experiments in [15] which suggest strong annealing of the displacement-damage-based trap type 1.

3. Simulation results and discussion

Using the refined modeling parameters for W and EUROFER outlined above, the T trapping probability $P_{\mathrm{Wall}}(t)$ was calculated for the different cooling concepts, wall fluxes, and EUROFER/Coolant boundary conditions similar to the approach in [1]. For all cases $P_{\mathrm{Wall}}(t)$ decreases with time because as the diffusion profile ($C_{\mathrm{Solute}}(x,t)$) propagates deeper, the diffusion flux ($\propto \nabla C_{\mathrm{Solute}}$) decreases. Thus, the uptake of T into the bulk, where it can be trapped at empty trap sites, is reduced. This effect is illustrated in figure 2(*a*) where an exemplary time evolution of the solute depth profile is plotted. The D concentration is shown as dotted graphs and, due to its slightly higher solute diffusion coefficient (mass difference w.r.t. T), it is slightly lower due to faster diffusion out of the two surfaces. The pronounced step at the interface at 0.8 (μm) is due to the different solubility of His in W and EUROFER. Due to the fast diffusion of His in EUROFER and low trap occupancy (see also figure 2(*b*)), permeation to the coolant sets in quickly after the solute diffusion profiles reaches the W/EUROFER interface.

The depth profiles of trapped T ($C_{\mathrm{Trapped}}(x,t)$) and D corresponding to the solute profiles in figure 2(*a*) are shown in figure 2(*b*). Most of the retention by trapping occurs in the W layer, trapping in EUROFER is negligible. This is particularly true for the HCPB cases with its higher wall temperature compared with WCLL. To calculate $P_{\mathrm{Wall}}(t)$ the total retained amount of trapped and solute $\delta^{\mathrm{T}}_{\mathrm{Ret}}\left(\mathrm{m}^{-2}\right)$ is calculated based on concentration profiles such as those shown in figure 2 using equation (2). $\rho(x)$ thereby is the number density (m^{-3}) of host atoms in either W (6.2×10^{28} m^{-3}) or EUROFER (8×10^{28} m^{-3}),

$$\delta^{\mathrm{T}}_{\mathrm{Ret}}(t) = \int \left(C_{\mathrm{Trapped}}(x,t) + C_{\mathrm{Solute}}(x,t)\right) \times \rho(x)\ \mathrm{d}x \qquad (2)$$

$P_{\mathrm{Wall}}(t)$ is then calculated by dividing $\delta^{\mathrm{T}}_{\mathrm{Ret}}\left(\mathrm{m}^{-2}\right)$ by total incident fluence $\theta^{\mathrm{T}}_{\mathrm{In}}\left(\mathrm{m}^{-2}\right)$ of T (see equation (1).

As explained in [1], based on a simple balance model, T-self-sufficiency is only possible when the wall losses described by $P_{\mathrm{Wall}}(t)$ are below a critical value $P^{\mathrm{Crit}}_{\mathrm{Wall}}$ given in equation (3)

$$P_{\mathrm{Wall}}(t) < P^{\mathrm{Crit}}_{\mathrm{Wall}} = (\mathrm{TBR} - 1)\,\frac{p_{\mathrm{Burn}}\left(\eta_{\mathrm{Pellet}} - R\left(\eta_{\mathrm{Pellet}} - \eta_{\mathrm{recycled}}\right)\right)}{\left(1 - p_{\mathrm{Burn}}\,\eta_{\mathrm{Pellet}}\right)}. \qquad (3)$$

In equation (3), p_{Burn} is the burn probability of T in the core, η_{Pellet} is the fuelling efficiency by pellets, η_{recycled} is the fuelling efficiency of T recycled at the wall, R is the fraction of the T wall flux that instantaneously recycles at the wall and TBR is the T-breeding ratio calculated for the blanket, neglecting wall

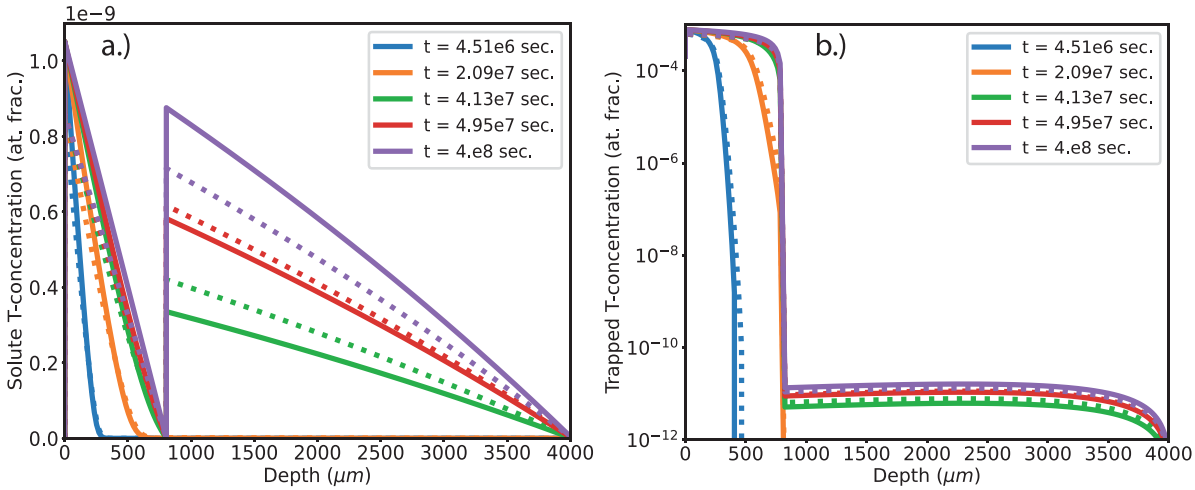

Figure 2. Time evolution of the T solute (*a*) and trapped (*b*) depth profiles for case 'HCPB0.8W3.2FE' with total influx of D and T of 1×10^{20} (m^{-2} s^{-1}) and diffusion limited boundary conditions at the EUROFER/Coolant interface. Dotted lines are the corresponding simulated D depth profiles.

Table 5. Upper and lower boundaries for parameter variations in equation (3) to estimate the expected range of $P^{\text{Crit}}_{\text{Wall}}$. The parameter ranges are based on the values used in [9].

Parameter	Lower boundary	Upper boundary
p_{Burn}	0.02	0.05
η_{Pellet}	0.3	0.8
η_{recycled}	0.001	0.05
R	0.99	0.9999
TBR	1.05 or 1.1	

losses. To obtain an estimate of the expected range for $P^{\text{Crit}}_{\text{Wall}}$ the parameters in equation (3) were varied as given in table 5.

In figure 3 a comparison of the time evolution of $P_{\text{Wall}}(t)$ from the TESSIM-X parameter scan with the required value of $P^{\text{Crit}}_{\text{Wall}}$ from the parameter scan of equation (3) (values according to table 5) is shown. For both parameter scans the resulting values were averaged to find the median value and the upper and lower boundaries of all samples in parameter scan. The refined predictions based on re-evaluated W simulation settings and new experimental/modeling results for EUROFER are very similar to the previous results from [1]. Depending on the TBR it takes on average between 1 and 2 FPYs to reach T-self-sufficiency. However, within the confidence interval for some cases no T-self-sufficiency is reached even within 6 FPYs. Those are low D, T wall flux WCLL cases where due to the lower temperature more T can be trapped and in combination with a lower wall flux it takes a long time until the traps are saturated.

The model for $P^{\text{Crit}}_{\text{Wall}}$ in [1] which is based on the work in [8, 9] has R, the fraction of His recycling at the first wall, as a free parameter. However, in reality R is not a free parameter. In the diffusion, trapping picture used to model the uptake and release with TESSIM-X, every HI that does not recycle via diffusion out of the plasma loaded surface instead diffuses into the bulk where it is trapped at defects or permeates to the coolant. Thus, R is a function of P_{Wall} and should be written $R = (1 - P_{\text{Wall}})$. Using this relation in the derivation of $P\,P^{\text{Crit}}_{\text{Wall}}$ in [1] leads to equation (4)

$$P_{\text{Wall}}(t) < {}^{*}P^{\text{Crit}}_{\text{Wall}} = \frac{\eta_{\text{recycled}}\, p_{\text{Burn}}\,(\text{TBR}-1)}{1+\eta_{\text{recycled}}\, p_{\text{Burn}}\,(\text{TBR}-1)-\eta_{\text{Pellet}}\, p_{\text{Burn}}\,\text{TBR}}. \tag{4}$$

This alternative description for $P^{\text{Crit}}_{\text{Wall}}$ in equation (4) yields very similar values for $P^{\text{Crit}}_{\text{Wall}}$ for the parameter range specified in table 5. The two models become identical for R as in equation (5)

$$R = \frac{1}{1-\frac{\eta_{\text{recycled}}(\text{TBR}-1)}{\eta_{\text{Pellet}}\,\text{TBR}-\frac{1}{p_{\text{Burn}}}}} \overset{p_{\text{Burn}}\ll 1}{\rightarrow} \frac{1}{1+\eta_{\text{recycled}}\,(\text{TBR}-1)\,p_{\text{Burn}}}. \tag{5}$$

From equation (5) follows that for the parameter values from table 5 the two models are identical for $0.99975 \leqslant R \leqslant 0.99998$. Only for very low ($\sim$0.99) values of R they differ. In figure 4 the two models for $P^{\text{Crit}}_{\text{Wall}}$ are compared with the 'refined' predictions for $P_{\text{Wall}}(t)$ similar to figure 3. Qualitatively the two models for $P^{\text{Crit}}_{\text{Wall}}$ do not differ significantly and the overlap with $P_{\text{Wall}}(t)$ is essentially the same.

Independent of the assumptions for describing $P^{\text{Crit}}_{\text{Wall}}$, only if the traps in the W armor layer are saturated to a sufficient depth, can the solute diffusion profile flatten further to reduce $P_{\text{Wall}}(t)$ below $P^{\text{Crit}}_{\text{Wall}}$. Therefore, it was proposed to pre-saturate the traps with H or D to avoid the need to saturate them with T [31]. However, in this proposal the effect of isotope exchange, which happens at all temperatures [17], is apparently neglected.

To show the effect of isotope exchange an exemplary calculation was performed for case 'HCPB0.8W3.2FE' (see table 1) with total influx of D and T of 1×10^{20} (m^{-2} s^{-1}) and diffusion-limited boundary conditions at the EUROFER/Coolant interface. The W and EUROFER layers

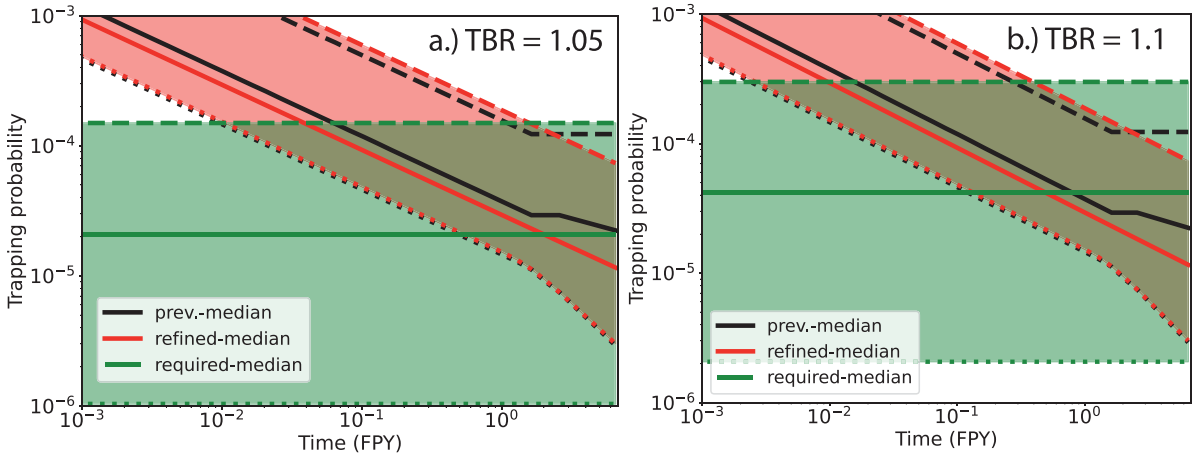

Figure 3. Overlap of 'previous' (from [1]) and 'refined' (this work) predictions for $P_{\mathrm{Wall}}(t)$ with the required value of $P_{\mathrm{Wall}}^{\mathrm{Crit}}$. (*a*) $P_{\mathrm{Wall}}^{\mathrm{Crit}}$ ranges from a parameter scan based on table 5 with TBR = 1.05, (*b*) $P_{\mathrm{Wall}}^{\mathrm{Crit}}$ ranges from a parameter scan based on table 5 with TBR = 1.1. The solid lines are the median values, the dashed and dotted graphs are the upper and lower boundaries, respectively.

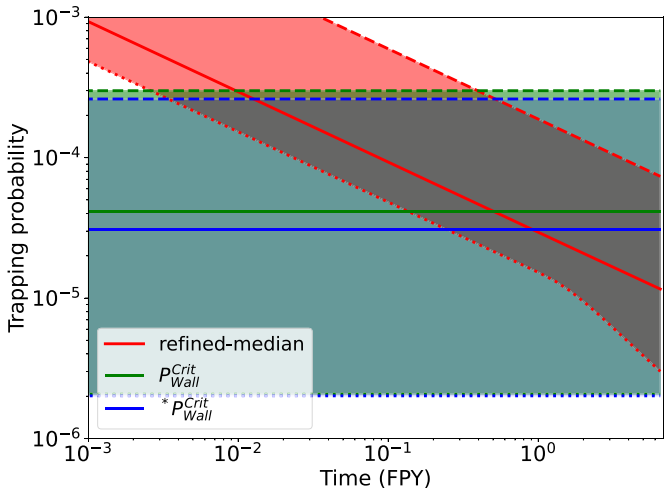

Figure 4. Comparison of the overlap of the 'refined' (this work) predictions for $P_{\mathrm{Wall}}(t)$ with the required value from the two different model descriptions for $P_{\mathrm{Wall}}^{\mathrm{Crit}}$ in equations (3) and (4). For a TBR = 1.1. The solid lines are the median values, the dashed and dotted graphs are the upper and lower boundaries, respectively.

are first saturated by a pure D flux and then again a 50:50 D:T mixed flux is applied.

In figure 5(*a*) the influence of pre-saturating the wall with D on the break through time of the T diffusion front to the coolant is shown. The curve 'Offset T-permeation' uses a shifted time axes which allows to compare the breakthrough of the T permeation through the empty sample 'No D-pre-loading T permeation' with the break through time of the T permeation for the pre-saturated wall. There is a small effect in that T reaches the coolant slightly faster but the resulting $P_{\mathrm{Wall}}(t)$ in figure 5(*b*) is almost indistinguishable from the value for T for the empty, un-saturated wall. This shows that isotope exchange does not alleviate the need for saturating the traps with T before T-self-sufficiency can be achieved. However, the faster T-break-through time makes it accessible earlier for recovery from the coolant.

Apart for the time needed the reduce the trapping probability to a value that allows T-self-sufficiency also the resulting total retained amount of T in the wall at any given time is of interest. From the TESSIM-X calculations the total retention (T m^{-2}) can be derived following equation (2). Assuming a first wall area of 1400 m^2, as was also used in [1], this can be converted to grams of retained T. In figure 6 the so calculated total retained amount of T [g] as function of time in FPY is shown. The predictions based on the refined model input are essentially identical to previous estimates in [1] and the retained amount reaches values of several 100 g of trapped T. These highest values are found for the WCLL concept at high wall fluxes: due to the low wall temperatures in WCLL concept more T is retained in the traps. Figure 6 only shows interval of all retention values encountered during the parameter scan, the highest retained amounts found for individual WCLL cases was up to ∼800 g. In contrast the individual cases for the higher temperature HCPB concept at most retain ∼200 g. Therefore, it can be concluded that a high first wall armor temperature is desirable to reduce retention.

In the current calculations the retention in EUROFER does not contribute significantly to the total retention despite the fact that volume wise it constitutes most of the first wall material. The results from [15] suggest annealing of displacement damage at the envisioned first wall operating temperatures $\gg$600 (K) and thus only the weak intrinsic traps remain which are hardly filled at these temperatures. However, this may be different when including the effect of the presence of He during displacement damage which would be present in EUROFER due to transmutation effects [32]. First preliminary results suggest that annealing in the presence of He is retarded.

To get a qualitative measure on how fast the retained T can be recovered from the wall after plasma off, figure 7 shows the decay of the retained fraction of T as function of time after plasma off i.e. $\Gamma_{\mathrm{In}} \rightarrow 0$. This was computed by first

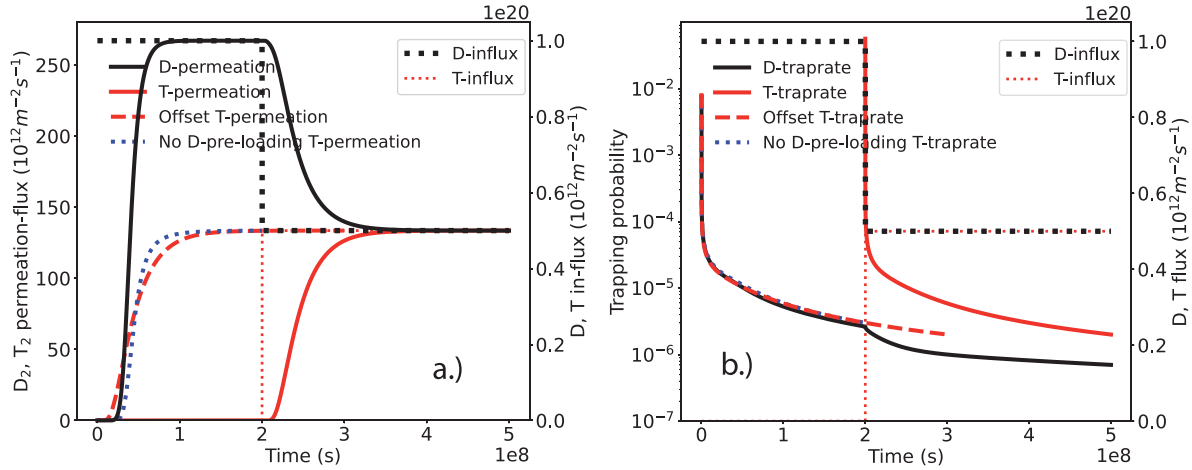

Figure 5. (*a*) Influence of isotope exchange on the break through time for T-permeation to the coolant and (*b*) influence of isotope exchange on the trapping probability $P_{\mathrm{Wall}}(t)$. Comparing the 'Offset' with the 'No D-pre-loading' curves shows the influence of pre-loading which due to effective isotope exchange at the high operating temperatures is negligible.

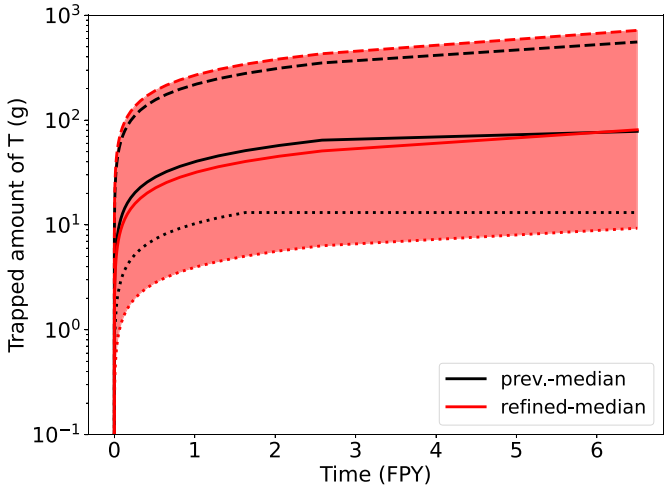

Figure 6. Comparison of the total retention vs. time for the previous predictions in [1] and the refined predictions (this work). The solid lines are the median values, the dashed and dotted graphs are the upper and lower boundaries, respectively.

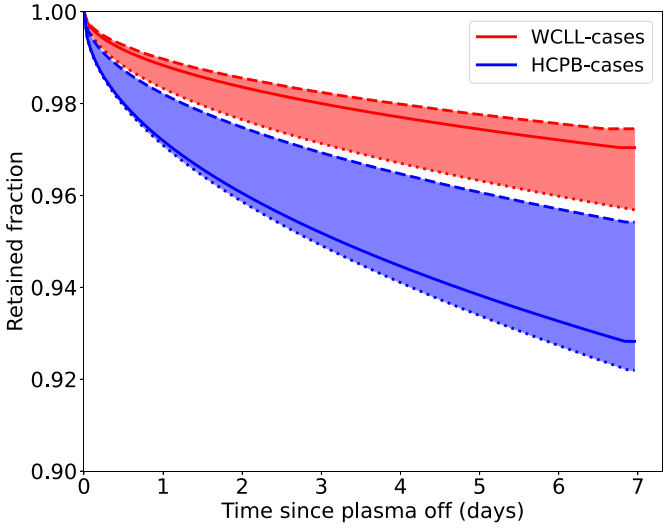

Figure 7. Fraction of T retained in the wall after plasma off for all considered cases in the parameter scan. The solid lines are the median values, the dashed and dotted graphs are the upper and lower boundaries, respectively. Note the suppressed 0 on the value axes.

loading the wall as before with a 50:50 D:T mixture for 10^8 s, then turning off the plasma but keeping the wall temperature constant. While keeping the wall temperature constant after plasma off is unrealistic, it provides an upper limit for the outgassed amount, since in reality the temperature will drop resulting in less T outgassing from the wall. The retained amount is followed for up to 7 d under these conditions and the so released amount is less than 10% in most cases. This is a consequence of the fact that most retention happens in the W armor with high de-trapping energies which only release D, T at temperatures above the foreseen first wall temperatures as can be seen from the TDS spectra in figure 1(*b*). Again, due to the higher operating temperatures the HCPB cooling concept releases more T than the WCLL. Still this plot shows that for either cooling concept, simply outgassing the wall is not a viable option to recover the T, since it would simply take a very long time.

4. Summary and conclusions

T-self-sufficiency is a key requirement for the operation of a future fusion reactor. However, current breeding blanket design studies underestimate the loss of T into the wall where it is stored in trap sites and recovery from the coolant is only possible after all trap sites are saturated with T and permeation into the coolant sets in. Based on current experimental data and benchmarked HI transport models the time evolution of the T wall loss rate $P_{\mathrm{Wall}}(t)$ can be estimated. A comparison of $P_{\mathrm{Wall}}(t)$ with a critical value $P_{\mathrm{Wall}}^{\mathrm{Crit}}$ required for T-self-sufficiency shows that it might take several FPYs before the wall is sufficiently saturated with T and the reactor becomes T-self-sufficient. However, large uncertainties remain in the input parameters for the models for $P_{\mathrm{Wall}}^{\mathrm{Crit}}$ and thus they span a very large range of approximately $10^{-6} \leqslant P_{\mathrm{Wall}}^{\mathrm{Crit}} \leqslant 10^{-4}$ where

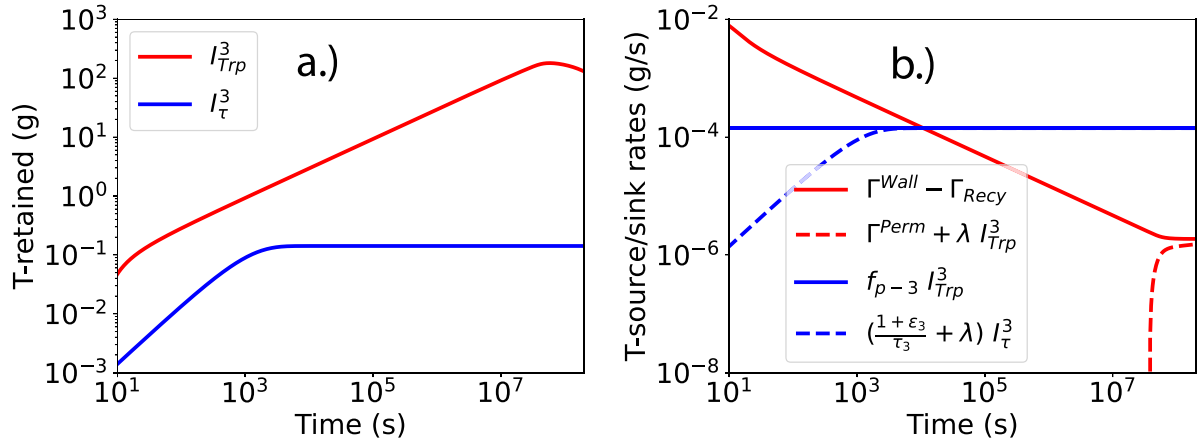

Figure 8. Comparison of the T retention in the main chamber wall based on diffusion trapping modeling from this paper with results based on equations and parameters from [33]. Figure (*a*) shows the time evolution of the total retained amount in the first wall and (*b*) shows the underlying source and sink rates as in equations (6) and (7). The residence time model graphs are blue, the diffusion tapping model graphs are red. In (*b*) the solid lines are the source and the dashed lines the sink-rates.

the lower value is obtained for the 'lower boundary'- and the upper value for the 'upper boundary' values in table 5. For an assumed first wall flux of $\sim 0.5 \times 10^{20}\,\mathrm{T(m^2 s)^{-1}}$ for a 50:50 D/T mixture in the incident wall flux this value range for $P^{\mathrm{Crit}}_{\mathrm{Wall}}$ corresponds to an allowable T loss rate between 0.03 and 3 g of T per day for a first wall area of 1400 $\mathrm{m^2}$. The dominant source for uncertainty in $P^{\mathrm{Crit}}_{\mathrm{Wall}}$ stems from the burn probability and fueling efficiencies. The underlying physics issues resulting in these uncertainties are discussed in section 6.2.1 in [33].

The models for T-self-sufficiency used in this publication to show the importance of the predicted T-trapping probabilities are rather simple. However, the results can also be used in more complete tritium fuel cycle models based on the residence time approach (see e.g. [33]). For instance, in the appendix of [33] the evolution of the T retention in the first wall $I^3_\tau\,(g)$ is described applying the residence time method in equation (A.3). If one neglects the influx of T form the heat exchanger and the coolant purification system and only takes the T-influx from plasma and T-loss to the heat exchanger into account, the following equation (6) remains for the T-content in the first wall. It is based on constant gain (f_{p-3}) and loss $\left(\frac{1+\epsilon_3}{\tau_3} + \lambda\right)$ rates, in particular the loss to the heat exchanger starts instantaneously,

$$\begin{aligned} \frac{\mathrm{d}I^3_\tau}{\mathrm{d}t} &= f_{p-3}\dot{T}_{\mathrm{i}} - \left(\frac{1+\epsilon_3}{\tau_3} + \lambda\right) I^3_\tau \\ f_{p-3} &= 10^{-4}, \tau_3 = 1000\,\mathrm{s}, \epsilon_3 = 0 \\ \lambda &= T - \text{decay rate}\left(\mathrm{s^{-1}}\right). \end{aligned} \tag{6}$$

This can be directly compared to the results in this publication which apply the diffusion trapping approach. The equation for the T-content I^3_{Trp} in the first wall is then based on the balance of fluxes $\left(\mathrm{m^{-2}\,s^{-1}}\right)$ into the plasma exposed surface Γ^{Wall}, the recycling flux back into the plasma $\Gamma^{\mathrm{Rec}}(t)$ and eventually after break through the permeation flux $\Gamma^{\mathrm{Perm}}(t)$ into the coolant. Thus, the net source (implantation flux Γ^{Wall} minus recycling flux $\Gamma^{\mathrm{Rec}}(t)$) and loss rates of T to the heat exchanger (the permeation flux $\Gamma^{\mathrm{Perm}}(t)$) are time dependent,

$$\begin{aligned} \frac{\mathrm{d}I^3_{\mathrm{Trp}}}{\mathrm{d}t} &= \frac{m_{\mathrm{T}}}{N_{\mathrm{A}}} A_{\mathrm{Wall}} \left(\Gamma^{\mathrm{Wall}} - \Gamma^{\mathrm{Rec}}(t) - \Gamma^{\mathrm{Perm}}(t)\right) - \lambda I^3_{\mathrm{Trp}} \\ A_{\mathrm{Wall}} &= 1400\mathrm{m^{-2}}, N_{\mathrm{A}} = \text{Avogadro number}, m_{\mathrm{T}} = 3\mathrm{g\,mol^{-1}}. \end{aligned} \tag{7}$$

Using the parameters from [33] in equation (6) and a T-injection rate $\dot{T}_{\mathrm{i}} = \frac{\dot{N}_{\mathrm{i}}}{\eta_{\mathrm{f}} f_{\mathrm{B}}}$ according to equation (3.5) in [33] for a T-burn rate $\dot{N}_{\mathrm{i}} = 459$ g $\mathrm{s^{-1}}$, burn fraction $f_{\mathrm{B}} = 1.5\%$ and fueling efficiency $\eta_{\mathrm{f}} = 25\%$ from table 1 in [33], allows to solve for the time evolution of the T content in the first wall I^3_τ. Similarly, using the fluxes calculated for the HCPB case with a total flux $0.5 \times 10^{20}\,\mathrm{T\ (m^2 s)^{-1}}$ of which only 44% (the rest is reflected) are implanted as Γ^{Wall} one can compute the total retention I^3_{Trp} by solving equation (7).

In figure 8 the resulting time evolution of the T contention in the first wall from diffusion trapping I^3_{Trp} and residence time modeling I^3_τ is compared. Also shown are the sources and sinks for the different approaches. The retention that builds up in the diffusion trapping picture is much larger because the sink to the heat exchanger only becomes active after permeation sets in which takes a long time $\sim$1 FPY. In contrast in residence time model the loss to the heat exchanger reaches its maximum value already after the T residence time in the first wall of 1000 s assumed in [33]. This result is also found for lower values of Γ^{Wall} for which initially both models yield similar time evolutions but after the residence time I^3_τ always falls behind I^3_{Trp} because permeation only sets in after break through is achieved for which all traps in the wall need to be

saturated. Thus, this comparison only confirms the conclusion drawn from the simple T-self-sufficiency models: saturating the bulk to reduce the T uptake results in much longer times until T-recovery becomes possible and the assumed residence time of $\tau_3 = 1000\,(\mathrm{s})$ is too short.

Based on first experiments trapping in displacement damaged EUROFER is small compared with W due to much stronger annealing of the defects created by the intense n-irradiation in EUROFER. However, the database is still limited, in particular data on trap site formation in the presence of He or during high temperature irradiation is needed since this can produce different defect types compared with irradiation at room temperature, which may not anneal so easily. The calculations include the effect of isotope exchange and show that pre-saturating the traps with D does not reduce the T-trapping rate during D/T operation. This means that the proposed 'Sponge Mechanism' [34] does not work because the required amount of T to saturate the traps remains the same.

Since T trapping is dominated by the W armor layer, the key design parameter is to minimize the W armor thickness in combination with high first-wall temperature to limit the amount of T that is needed to saturate the first-wall trap sites. Within the limits introduced by erosion lifetime the current 'optimum design' w.r.t. T-self-sufficiency is therefore the HCPB cooling concept with a 0.8 mm W armor layer. Based on this 'optimum design' the maximum value of $P_{\mathrm{Wall}}^{\mathrm{Crit}} = 10^{-4}$ is reached after $\sim$2 weeks. In contrast, for the worst design w.r.t. T-self-sufficiency, the WCLL cooling concept with a 2 mm W armor layer it is only reached after $\sim$4 years. However, the burn rate and fueling rate remain rather uncertain, see also [33] and therefore the value $P_{\mathrm{Wall}}^{\mathrm{Crit}} = 10^{-4}$ may simply be too optimistic. As can be seen from lower values of $P_{\mathrm{Wall}}^{\mathrm{Crit}}$ take significantly longer to reach.

Overall, the goal has to be to avoid the need for saturating the bulk to reduce the T uptake, but to increase the release of T through the plasma-facing surface. Since a further reduction of the W armor layer is probably impossible due to erosion lifetime limitations, this could be achieved by castellating the surface by introducing closely spaced gaps. The diffusion out of the side surfaces of these gaps would stop the permeation of T into the bulk and lead to outgassing back into the plasma. The width of the castellations however would have to be significantly smaller than the W armor thickness for this approach to alleviate the T-self-sufficiency challenges introduced by trapping T in the wall. Therefore, such castellations are probably technically not feasible. Another option is open porosity which would act similarly to the surface castellation: T diffusing into the open cavities would simply outgas from the surface. Open porosity can either be introduced by the armor layer manufacturing process [35] or by the impinging He. According to [36] the admixture of He reduces the permeation flux probably by open porosity introduced by a dense He bubble network close to the surface.

Independent of the possible mitigation processes the T-cycle modeling efforts need to take the increased losses of T in the first wall due to n-damage induced defects into account.

Acknowledgments

This work has been carried out within the framework of the EUROfusion Consortium, funded by the European Union via the Euratom Research and Training Programme (Grant Agreement No. 101052200 â EUROfusion). Views and opinions expressed are however those of the author(s) only and do not necessarily reflect those of the European Union or the European Commission. Neither the European Union nor the European Commission can be held responsible for them.

ORCID iDs

T. Schwarz-Selinger https://orcid.org/0000-0001-7461-2817
R. Arredondo https://orcid.org/0000-0002-6802-8523

References

[1] Arredondo R., Schmid K., Subba F. and Spagnuolo G.A. 2021 *Nucl. Mater. Energy* **28** 101039
[2] Fischer U. *et al* 2017 *Fusion Eng. Des.* **123** 26
[3] Carella E., Moreno C., Urgorri F.R., Rapisarda D. and Ibarra A. 2017 *Fusion Eng. Des.* **124** 687
[4] Franza F., Boccaccini L.V., Fable E., Landman I., Maione I.A., Petschanyi S., Stieglitz R. and Zohm H. 2022 *Nucl. Fusion* **62** 076042
[5] Cismondi F. *et al* 2020 *Fusion Eng. Des.* **157** 111640
[6] Klimenkov M., Jäntsch U., Rieth M., Dürrschnabel M., Möslang A. and Schneider H.C. 2021 *J. Nucl. Mater.* **557** 153259
[7] Day C., Butler B., Giegerich T., Ploeckl B. and Varoutis S. 2019 *Fusion Eng. Des.* **146** 2462
[8] Doerner R., Tynan G.R. and Schmid K. 2019 *Nucl. Mater. Energy* **18** 56
[9] Tynan G.R., Doerner R.P., Barton J., Chen R., Cui S., Simmonds M., Wang Y., Weaver J.S., Mara N. and Pathak S. 2017 *Nucl. Mater. Energy* **12** 164
[10] Federici G., Biel W., Gilbert M.R., Kemp R., Taylor N. and Wenninger R. 2017 European DEMO design strategy and consequences for materials *Nucl. Fusion* **57** 092002
[11] Brezinsek S. *et al* 2017 *Nucl. Fusion* **57** 116041
[12] Zibrov M., Dürbeck T., Egger W. and Mayer M. 2020 *Nucl. Mater. Energy* **23** 100747
[13] Pečovnik M., Schwarz-Selinger T. and Markelj S. 2021 *J. Nucl. Mater.* **550** 152947
[14] Markelj S., Schwarz-Selinger T., Pečovnik M., Chrominski W., Šestan A. and Zavašnik J. 2020 *Nucl. Fusion* **60** 106029
[15] Schmid K., Schwarz-Selinger T. and Arredondo R. 2023 *Nucl. Mater. Energy* **34** 101341
[16] Ogorodnikova O., Zhou Z., Sugiyama K., Balden M., Pintsuk G., Gasparyan Y. and Efimov V. 2017 *Nucl. Fusion* **57** 036011
[17] Schmid K., Von Toussaint U. and Schwarz-Selinger T. 2014 *J. Appl. Phys.* **116** 134901
[18] Schmid K. and Zibrov M. 2021 *Nucl. Fusion* **61** 086008
[19] Martelli E. *et al* 2018 *Int. J. Energy Res.* **42** 27
[20] Hernández F., Pereslavtsev P., Kang Q., Norajitra P., Kiss B., Nádasi G. and Bitz O. 2017 *Fusion Eng. Des.* **124** 882
[21] Frauenfelder R. 1969 *J. Vac. Sci. Technol.* **6** 388
[22] Aiello A., Ricapito I., Benamati G. and Valentini R. 2002 *Fusion Sci. Technol.* **41** 872

[23] Holzner G., Schwarz-Selinger T., Dürbeck T. and Toussaint U.V. 2020 *Phys. Scr.* **T171** 014034
[24] Schmid K., Schwarz-Selinger T. and Theodorou A. 2023 *Nucl. Mater. Energy* **36** 101494
[25] Behrisch R., Federici G., Kukushkin A. and Reiter D. 2003 *J. Nucl. Mater.* **313–316** 388
[26] Kocan M., Gennrich F.P., Kendl A. and Müller H.W. 2012 *Plasma Phys. Control. Fusion* **54** 085009
[27] Mutzke A. *et al* 2019 SDTrimSP Version 6.00 (IPP 2019–02) (Max-Planck-Institut für Plasmaphysik) (https://doi.org/10.17617/2.3026474)
[28] Markelj S., Schwarz-Selinger T., Pečovnik M., Založnik A., Kelemen M., Čadež I., Bauer J., Pelicon P., Chromiński W. and Ciupinski L. 2019 *Nucl. Fusion* **59** 086050
[29] Pečovnik M., Hodille E.A., Schwarz-Selinger T., Grisolia C. and Markelj S. 2020 *Nucl. Fusion* **60** 036024
[30] Hodille E.A., Ferro Y., Fernandez N., Becquart C.S., Angot T., Layet J.M., Bisson R. and Grisolia C. 2016 *Phys. Scr.* **2016** 014011
[31] Deng B., Li Z., Huang J. and Yuan T. 2004 *Fusion Sci. Technol.* **64** 548
[32] Gilbert M.R., Dudarev S.L., Zheng S., Packer L.W. and Sublet J.-C. 2012 *Nucl. Fusion* **52** 083019
[33] Abdou M., Riva M., Ying A., Day C., Loarte A., Baylor L.R., Humrickhouse P., Fuerst T.F. and Cho S. 2021 *Nucl. Fusion* **61** 013001
[34] Deng B., Li Z.X., Li C.Y. and Feng K.M. 2011 *Nucl. Fusion* **51** 073041
[35] Greuner H., Bolt H., Böswirth B., Lindig S., Kühnlein W., Huber T., Sato K. and Suzuki S. 2005 *Fusion Eng. Des.* **75–79** 333
[36] Ueda Y., Lee H.T., Peng H.Y. and Ohtsuka Y. 2012 *Fusion Eng. Des.* **78** 1356